A novel cylindrical bonnet tool polishing method for bearing ring internal surface finishing

Zhenyu Jiang[a], Chen Jiang[a], Jiahao Liu[a], Xun Chen[b], Lingxin Shen[a], Rui Gao[a]

a *College of Mechanical Engineering, University of Shanghai for Science and Technology, Shanghai, 200093, China*

b *General Engineering Research Institute, Liverpool John Moores University, Liverpool L3 3AF, UK*

Abstract: Traditional bonnet tool polishing (BTP) method is an efficient and controllable processing technology for plane, spherical and aspherical surfaces, but this method cannot process the internal surface of cylindrical workpiece. This paper proposes a novel cylindrical bonnet tool polishing (CBTP) method for the internal surface of the bearing ring. The CBTP method uses a self-developed cylindrical bonnet tool with small size, and abrasive slurry is used to polish the internal surface of the part. The characteristics of the contact area is firstly analyzed through a finite element analysis (FEA) simulation. After that, a series of single factor polishing experiments are conducted to investigate the effect on surface roughness and material removal. The results show that combining rotation and reciprocating motions can improve surface roughness and increase the amount of material removal simultaneously. Higher air pressure and proper tool offset is conducive to improve surface roughness and polishing efficiency. Moreover, relatively high material removal and better surface roughness can be obtained under longer polishing time and faster rotation speed. The surface roughness can be achieved 0.0265μm by using the combination of 1μm SiC and 0.5μm CeO_2 particles.

1 Introduction

Bearing is one of the most widely used elements in rotating machines, which plays an important role in the modern manufacturing industry [1]. As a critical component of the bearing, bearing ring need to undergo heat treatment, milling, grinding and hard turning processing. Nevertheless, a high surface roughness value and fatigue cracks are inevitable due to the nature of the manufacturing process [2-3]. These defects on the contact surface can easily affect the formation of lubricating oil films and significantly influence the bearing fatigue life performance [4]. At present, oilstone high-frequency oscillation is generally used as the last step to finish the contact surface, which easily leads to micro scratches and limits the improvement of surface quality [5]. Therefore, it is of great practical significance to find an efficient manufacturing technique to finish the contact surface.

The contact surface that needs to be finished of a rolling bearing covers two aspects: (i) outer contact surface of the internal bearing ring and (ii) internal contact surface of the outer bearing ring. Currently, some polishing technologies have been successfully applied in polishing the outer contact surface, including shearing-thickening polishing(STP) [6-8], Floating abrasive polishing(FAP) [9] and electrochemical mechanical polishing(ECMP) [10-11]. However, compared to the outer contact surface, polishing of the internal contact surface is extremely challenging due to the geometric limitations of conventional machining tools [12]. Mccarty [13] developed a technique in 1970s as known as abrasive flow machining(AFM), which is capable of polishing internal surfaces by using a self-deforming tool under the assistance of two hydraulically operated cylinders. Wu et al. [14] presented a

research on the precision polishing of the internal surface of a large size bearing ring by AFM, which eventually reduce the surface roughness and change the surface microstructure and texture. Brar et al. [15] used AFM to polish the internal surface of a hollow cylindrical workpiece and found that the roundness increased by 46.83% and the surface roughness reduced by 47.83%. However, in the process of AFM for the internal surfaces, there are some limitations include abrasive agglomeration, nonuniform surface finishing due to machine vibration and low efficiency [16]. Except for the above-mentioned processing methods, magnetic field assist polishing (MFAP) is also considered to have great potential for internal surface machining [17-18]. Zhen et al. [19] devised a novel magnetorheological polishing(MRP) process to polish the internal surface of titanium alloy tubes. Song et al. [20] also used MRP technology to achieve micro-level polishing of the internal surface of the cylindrical workpiece. Chen et al. [21] investigated a new type of magnetic hot melt adhesive particles(MHMA) for spiral polishing on the inner wall, however, the magnetorheological media are complex and costly to prepare. Therefore, development of a new polishing technique for the bearing ring internal surface should overcome the limitations such as low efficiency, environmental unfriendly and inconsistent surface finish. Bonnet tool polishing (BTP) was introduced by Walker for the first time, it used an inflated spherical membrane as the polishing tool and is able to confirm with various local curvature [22]. Nowadays, this technique has become more commonly used in recent years as a high efficiency and controllability polishing technology for hard and brittle materials [23-28]. However, traditional BTP is not suitable to polishing the complex internal surface.

In this paper, a novel cylindrical bonnet tool polishing (CBTP) method was developed to polish the internal surface of a GCr15 steel ring by using a self-developed polishing machine. Firstly, the working principle of the CBTP method was introduced. After that, a series of simulation studies of contact area characteristics via finite element analysis (FEA) are undertaken, and the range of values of key factors was also explored. Furthermore, single factor experimental verifications were executed on evaluating the polishing performance of the CBTP method, together with the discussions and conclusions of the paper.

2 Methodology

2.1 The CBTP tool and polishing principle

In order to process the cylindrical internal surface, miniaturization of the bonnet tool should be carried out and retaining the adaptability of the traditional bonnet tool. There are two main issues that need to be considered in the miniaturization process, which are the design of the CBTP tool and the renewal of the polishing principle. The concept of the novel bonnet polishing tool is shown in Fig.1(a)-(c). A small cylindrical bonnet of rubber material with 20mm outer diameter and 25mm length is used as the polishing tool. The tool surface is attached with polyurethane polishing pad by the glue and fixed on the polishing handle by a nut, as shown in Fig.1(b). During processing, the polishing tool is filled with gas and it can expand appropriately under the action of internal air pressure. For the purpose of dissipating heat and transporting the polishing slurry, the surface of the polishing pad was provided with a cross-shaped groove of a certain width. When the slurry was released onto the tool surface, abrasives contained in the slurry will embedded on the polishing pad due to its pore-shaped

surface texture and the abrasives on the polishing pad were checked by a digital microscope (VHX-6000). Sharp edges of abrasives on the tool surface were observed in Fig.1(c). In this way, the CBTP tool can use the sharp edges of abrasives to process the internal surfaces.

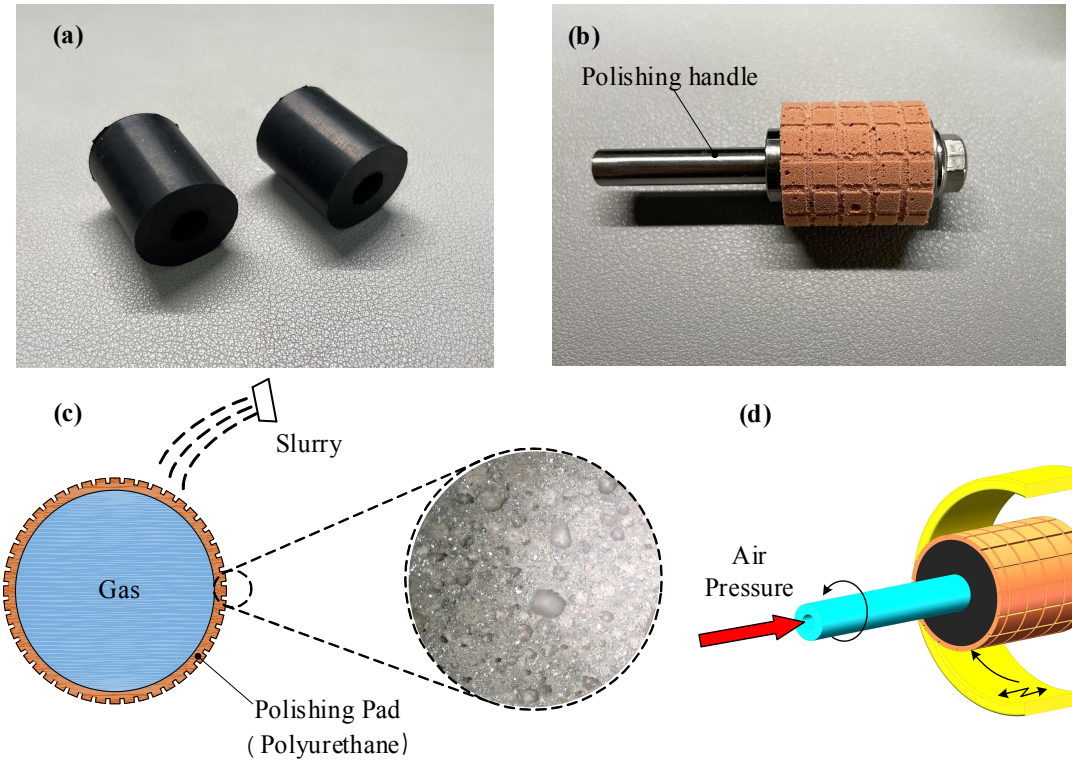

Fig.1 (a) Rubber material CBTP tool. (b) Installed CBTP tool. (c) Schematic diagram of the proposed CBTP tool. (d) Schematic diagram of the CBTP polishing principle.

Regarding to the BTP method, the rotation-axis of the tool inclined to the surface's local normal at an angle of 10-15 degrees. Then, the tool axis forms a 'Precession' movement around the local normal to the surface of the flat or aspherical parts [29]. Compared to the traditional BTP technology, Fig.1(d) depicted the schematic diagram of the CBTP polishing principle. The proposed CBTP tool is insert into the workpiece, air with a certain pressure is charged into the tool by compressor through the polishing handle and make it fully contact with the internal surface. When contact occurs, the force acting on the abrasives exert polishing force on the internal surface, and the inner air pressure and the tool offset can be adjusted to change the polishing force. Under the polishing force, the sharp edges of abrasive particles will scratch the workpiece. Subsequently, the tool makes a high-speed rotational movement in reverse with the workpiece driven by the spindle, and then, in order to obtain a homogeneous internal surface, a reciprocating linear motion of the workpiece within a certain interval is also added at the same time. Under the coupling of the above three motions, the polishing tool forms a machining path similar to honing, the whole internal cylinder surface can be polished.

2.2 Concept of the experimental setup

The experimental setup is designed to explore the methods and devices for the CBTP process on the cylindrical internal surfaces, which can provide both automated processing process and flexible process selection. The developed experimental setup is a four-axis

polishing machine, which contains two linear slide table and two rotary axes, as shown in Fig.2. The polishing spindle is installed on the *Y* direction linear slide table and the polishing tool is installed on the polishing spindle by means of a precision collet. The polishing spindle is driven by a servo motor with a maximum speed of 8000rpm. The workpiece is fixed by the fixture and driven by a servo motor. A three-dimensional force sensor is mounted under the fixture base to measure the polishing force in normal and tangential directions. In addition, all the servo motors in the polishing machine are all driven by the drivers through PLC (SIEMENS S7-1200) to precisely control the rotational speed. The slurry circulation system consists of a pump, a mixer and a nozzle. Since the polishing slurry is a mixed medium, consists of deionized (DI) water and abrasive particles. To ensure the uniformity of abrasive particles in the polishing slurry, the mixer needs to keep rotating during polishing process. The diaphragm pump uses the internal pressure difference to transport the polishing slurry to the nozzle and spray onto the surface of the polishing tool. On the other hand, a recycling container is fixed under the workpiece, and the polishing slurry is recycled into the storage tank to achieve green circulation.

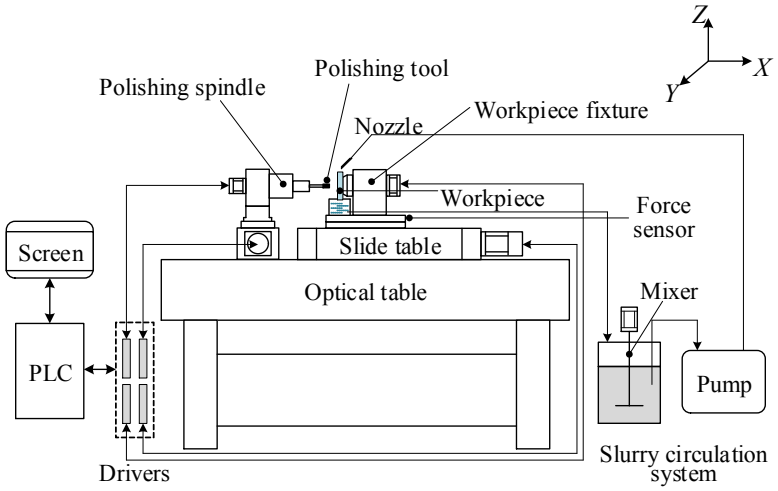

Fig.2 Schematic diagram of the novel CBTP machine

3 Analysis of contact area through FEA simulation

3.1 Simulation modeling

With the development of the FEA (Finite Element Analysis) simulation, it has become an effective approach for the contact simulation. In this paper, due to the elasticity of the polishing tool, the nonlinear contact status will occur when the tool contacting with the workpiece, which affects the controllability of the polishing results. Therefore, it is important to analyze the influence of key factors on the features of the contact area through FEA simulation. Here, the features of the contact area consist of the shape and pressure distribution of the contact area. The simulation was conducted between bearing steel (GCr15) and rubber material, which are hard and nonlinear material respectively. Fig.3(a) shows the CBTP geometric model in ANSYS 19.0 software, which was meshed with high-resolution hexahedral mesh and only half of the workpiece is displayed for the convenience of observation. Moreover, because the contact occurs on the workpiece surface, the mesh must

be refined in the internal target surface to enhance the computational precision. The total number of meshes was 161682. The outer diameter of the workpiece is 45mm, the inner diameter is 40mm and width is 17mm, tool size is as described in Section 2. Furthermore, key selection factors include inner air pressure(p) and tool offset(h), the values of which are set from 0.05MPa to 0.3MPa and changes from 0.05mm to 0.3mm. Fig.3(b) shows the total deformation and contact status of the simulation model.

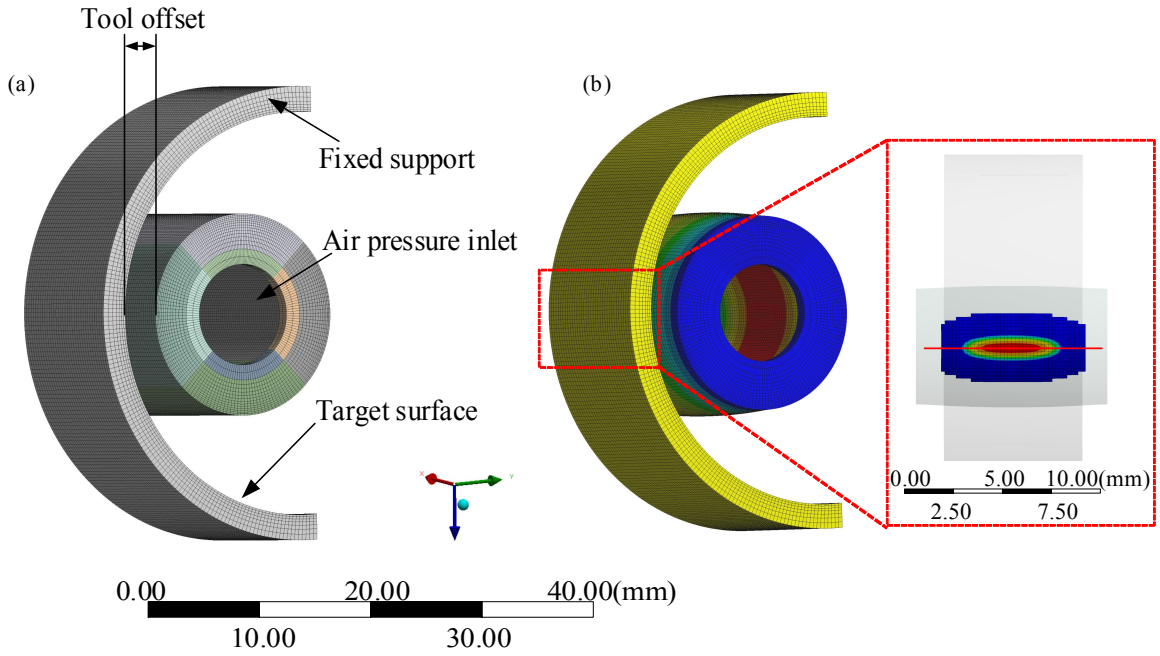

Fig.3 The simulation model and contact status in ANSYS software

3.2 Simulation results and analysis

Fig.4 and Fig.5 shows the simulation results of the contact model in the contacting area. Fig.4(a) shows the changes of the shape of the contact area under different tool offset h. It is interesting to find that the shape and area of the contacting area become irregular and larger with the increase of the tool offset h. When the tool offset $h \leqslant 0.15$mm, the contact area is oval shape and regular; but when the $h > 0.15$mm, the contact area gradually becomes a rectangle and the center obviously become concave. The concave in the contact area will affects the contact between abrasives and workpiece surface. On the other hand, the changes in maximum value and average value of the contact pressure under different tool offset h is shown in Fig.4(b) with lines. The graph shows that there has been a steady increase of the average value from 0.0002MPa to 0.05MPa, but in contrast, the maximum pressure value has a steep rise from 0.04MPa to 0.25MPa. Fig.4(c) shows the contact pressure distribution extracted along the red section line in Fig.3(b). It is also found that when $h \leqslant 0.15$mm, the pressure distribution is regular, symmetric and Gaussian-like, and when $h > 0.15$mm, the pressure distribution become irregular. To sum up, tool offset h will impact the area and shape of the contact area, the value and distribution of the contact pressure. These analyses further inferred that to ensure a stable and adequate contact between the polishing tool and workpiece, the tool offset h should be selected under 0.15mm.

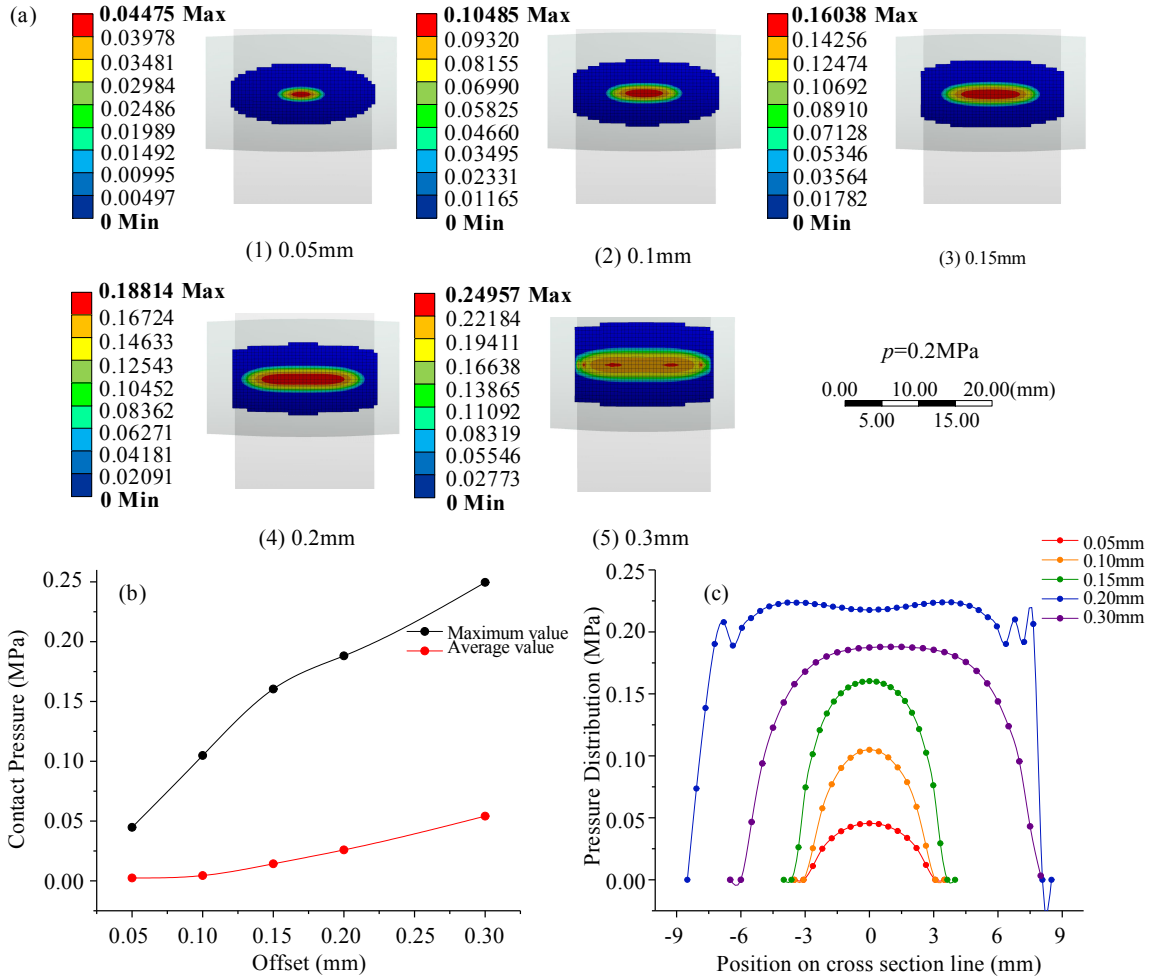

Fig.4 Simulation results of the contact model in the contacting area: (a) changes of the shape of the contact area under different tool offset h, (b) contact pressure value under different tool offset h, (c) contact pressure distribution under different tool offset h.

To find how the inner air pressure p impacts the features of the polishing footprint, the inner air pressure p is set to be 0.05MPa, 0.1MPa, 0.15MPa, 0.2MPa and 0.3MPa respectively, then the tool offset h is set to be 0.15mm. The simulated results are shown in Fig.5. When the inner air pressure $p \leqslant 0.15$MPa, the shape of the contact area is irregular and rectangle. This is due to the fact that the internal pressure is too low, so that the rubber material cannot expand uniformly. When contact occurs, the two sides of the cylindrical tool are deformed first, and the center of the tool is dented. As can also be seen from Fig.5(b), the average contact pressure remained stable across all inner air pressure p, but the maximum decreased from 0.71598 MPa to a low of 0.20763MPa. When the p-value exceeded 0.15MPa, the maximum pressure gradually increased. The pressure distribution is also extracted and lined in Fig.5(c). As shown in Fig.5(c), the pressure distribution is irregular and non-Gaussian-like when the air pressure less than or equal to 0.15MPa. However, when p-value greater than 0.15MPa, stress distribution become regular, symmetric and Gaussian-like because of the polishing tool properly inflated under the action of inner air pressure.

Based on the above simulation results and analysis, the tool offset h and inner air pressure p are key factors affecting the shape of the contact area, the symmetry of the pressure

distribution and the pressure value, which are closely related to the polishing experiments below. In subsequent studies, the value range will set to be 0.1mm < h < 0.15mm, and p > 0.2MPa.

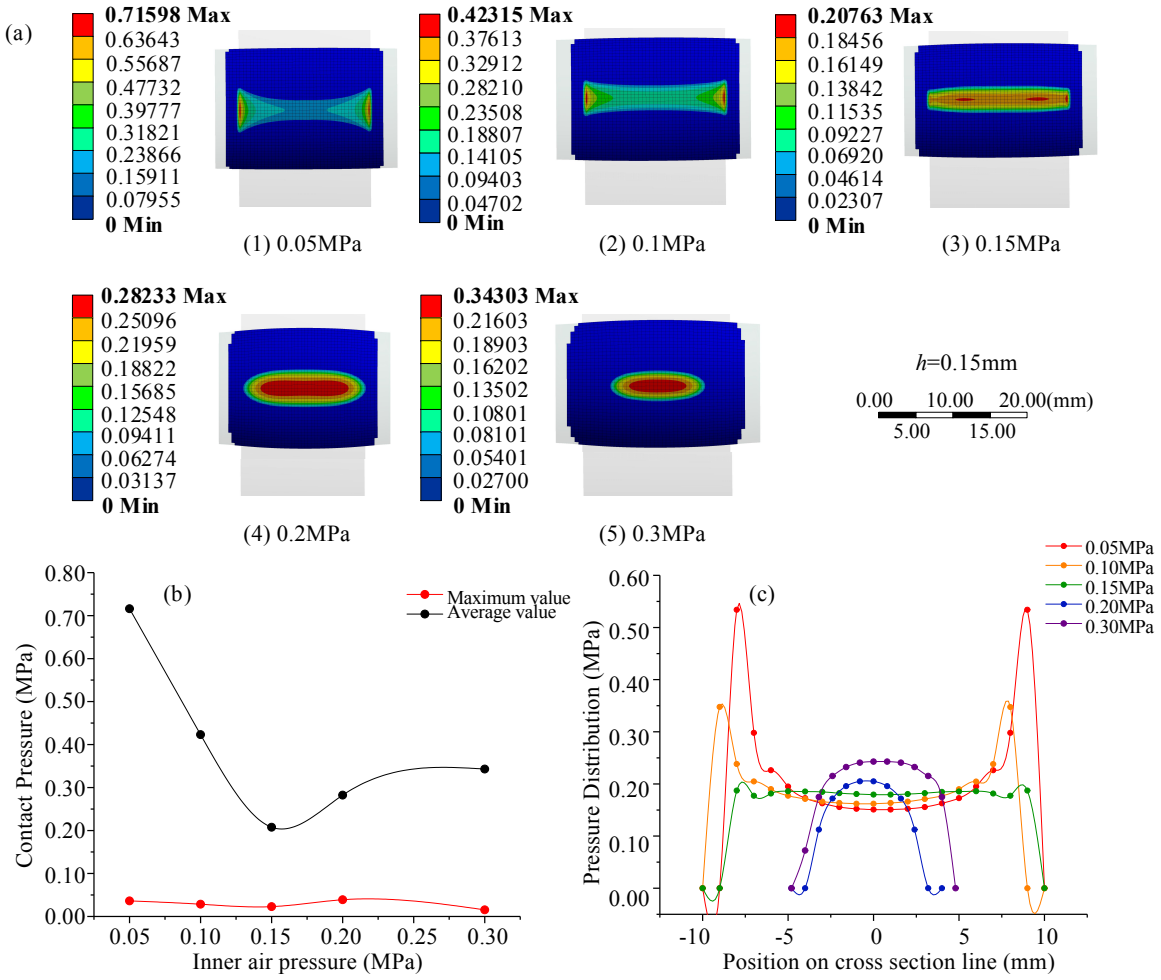

Fig.5 Simulation results of the contact model in the contacting area: (a) changes of the shape of the contact area under different inner air pressure p, (b) contact pressure value under different inner air pressure p, (c) contact pressure distribution under different inner air pressure p.

4 Experimental setup and conditions

Corresponding to the concept in Sec.2, the experiments were conducted on a self-developed CBTP polishing machine. The overall and zoom-in details of the polishing machine are shown in Fig.5. The tested workpiece was a ring with 45mm outer diameter, 40mm inner diameter and 17mm width. Furthermore, the intelligent control system was shown in the upper part of Fig.5(b), the internal air pressure of the CBTP tool and the power of the slurry circulation system in Fig.5(c) were both provided by the compressor in the lower part of Fig.5(b).

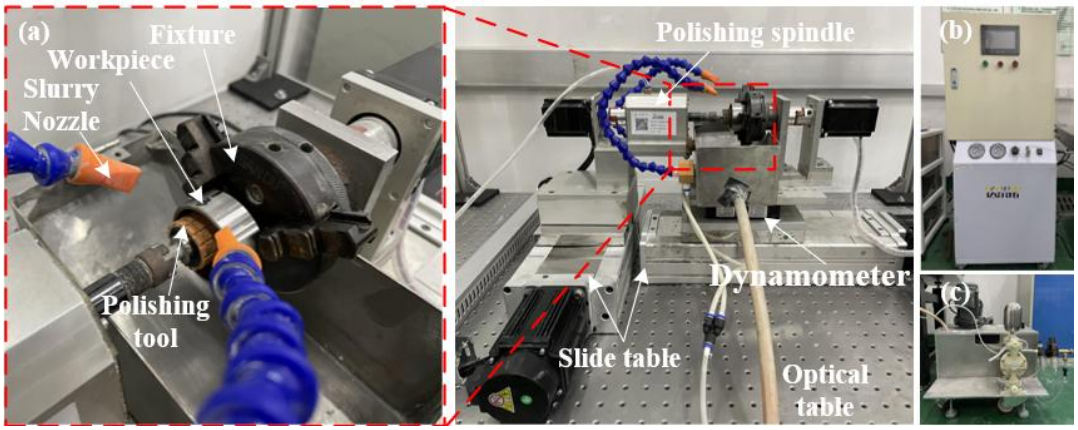

Fig.5 (a) the experimental setup, (b) the intelligent control system (upper) and compressor (lower), (c) the polishing slurry circulation system.

To explore the effect of the CBTP parameters on the surface roughness and material removal amount of the workpiece, five groups of single-factor experiments were designed. The single-factors and different experimental details for each group were summarized in Table1. As for group 3, the total polishing time is 15mins and after every 3mins interval, the workpiece was cleaned and evaluated. Moreover, five combinations of abrasives were prepared for group 6, which are 1μm SiC, 1μm CeO_2, 0.5μm and 1μm SiC, 0.5μm and 1μm CeO_2, 0.5μm CeO_2 and 1μm SiC respectively. It is worth noting that, the last three sets of experiments in group 6 were performed with segmented polishing consisting of different sizes of abrasives. The rotation speed for each phase was 1500 and 500rpm respectively. Other experimental parameters were shown in Table 2.

Table 1 Grouping of the CBTP single-factor experiments

Group	Factors	Details
1	Motion modes	0.2Mpa, 0.15mm,1500rpm and polished 3mins
2	Air pressure and tool offset	0.15mm at different air pressures, 0.2Mpa at different tool offset and polished 3mins
3	Polishing time	0.2Mpa, 0.15mm,1500rpm
4	Tool rotation speed	0.2Mpa, 0.15mm,1500rpm and polished 3mins
5	Abrasive types and size	0.2Mpa, 0.15mm and polished 12mins

Table 2 Experimental conditions

Polishing parameters (unit)	Value
Motion modes	Rotation, Rotation and reciprocating
Tool air pressure (MPa)	0.05, 0.1, 0.15, 0.2, 0.3
Tool Offset (mm)	0.05, 0.1, 0.15, 0.2, 0.3
Polishing time (min)	3~15
Tool rotational Speed (rpm)	500, 1000, 1500, 2000
Abrasive types	SiC, CeO_2
Abrasive size (μm)	0.5, 1
Slurry concentration (%)	5

After each group of experiments were finished, the workpiece was cleaned with ethanol in an ultrasonic cleaner and dried by hot air. After that, the workpieces were average cutting by wire EDM, and the polished surface was evaluated using a profilometer (Form Talysurf 200) and a confocal microscope (usurf explorer). The material removal amount was weighted by an electronic balance (resolution 0.01mg). Moreover, in order to ensure adequate statistical accuracy, each group of experiments was repeated 3 times.

5 Results and discussion

5.1 Surface topography and roughness

The results of the surface roughness under different motion modes were summarized in Fig.6. As shown in Fig.6(a), the surface roughness under rotation motion was improved from 0.725μm Ra to about 0.373μm Ra, reduced by 48.5%. Nevertheless, as seen in Fig.6(d), the roughness under combining rotation and reciprocating motions was improved to about 0.074μm Ra in 3mins, reduced by about 90%.

Fig.6(b) and (e) present the profile of the polished area under rotation motion and combining rotation and reciprocating motion by using a profilometer respectively (Form Talysurf 200). As the rotation motion is unique in the circumferential direction, the abrasive particles are only to polish along the original scratches. On the other hand, when reciprocation is added to the rotation motion, the abrasive particles are able to polish the surface in the direction along and perpendicular to the scratch simultaneously, which significantly improve the depth of material removal. Fig.6(c) and Fig.6(f) show the surface morphology transition between rotation motion and combining rotation and reciprocating motion under a confocal microscope (usurf explorer). It can be seen that there were a few dense scratches on the polished surface under rotation motion and it still preserves high asperities and low valleys. In contrast, when using a combination of rotation and reciprocating motion, the polished surface quality is more uniform and the number of scratches is also obviously reduced.

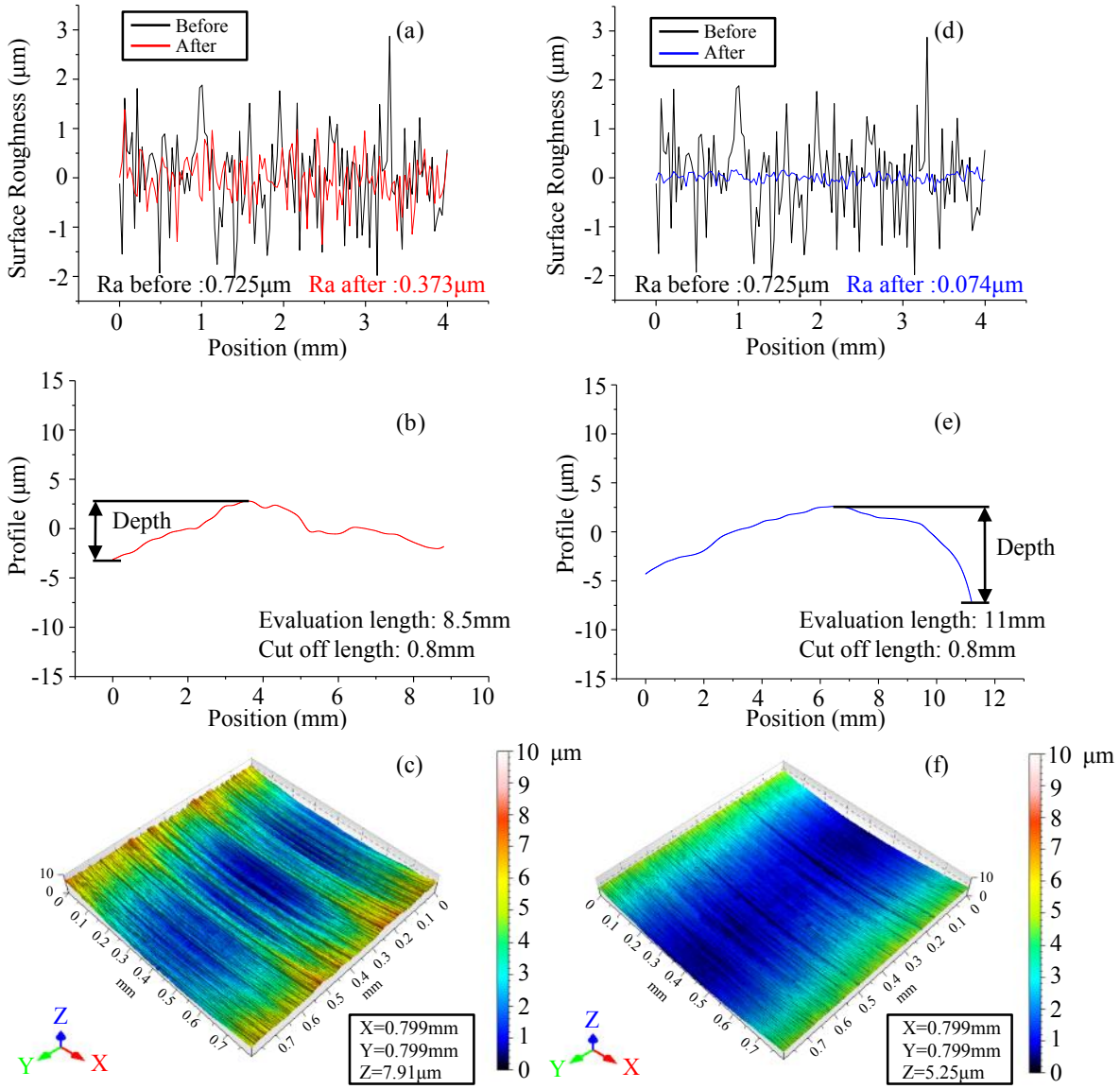

Fig.6 Comparison of polishing results under different motion modes: (a) surface roughness under rotation motion, (b) polished profile under rotation motion, (c) surface microscope view under rotation motion, (d) surface roughness under combining rotation and reciprocating motion, (e) polished profile under combining rotation and reciprocating motion and (f) surface microscope view under combining rotation and reciprocating motion.

5.2 Effect of air pressure *p* and tool offset *h*

Fig.7 demonstrates the influence of the air pressure *p* and tool offset *h* on the polishing results. In Fig.7(a), when the air pressure changed from 0.05MPa to 0.3MPa, the surface roughness improved from 0.097μm to 0.046μm, however, the material removal increased from 2.88mm^3 to 11.17 mm^3. Based on the simulation results, we infer that the likely reason is that with the increase of the air pressure, as well as increasing the force exerted by abrasives on the workpiece surface, and the scratch-removal capability becomes stronger and the amount of material removal increases. In the case of variable tool offset experiment, the surface roughness improved from 0.079μm to about 0.055μm and surface roughness did not

change significantly after 0.1mm. Furthermore, material removal results also show a large increase after 0.1mm, this trend is hypothesized to be due to the increase in contact area caused by the increase of tool offset, which rises the amount of abrasives involved in the polishing in the contact area and the increase in polishing force of a single abrasive particle, which is consistent with the simulation results.

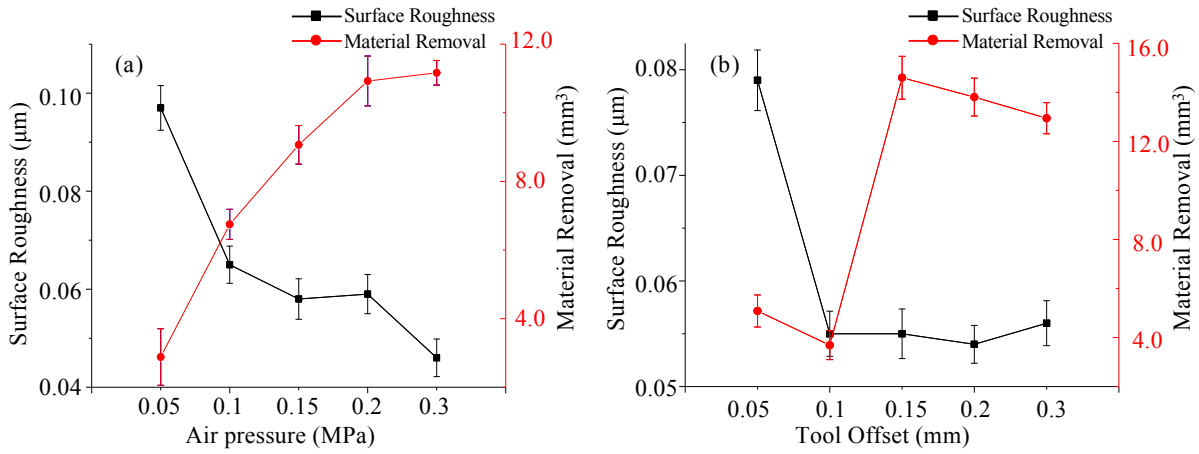

Fig.7 Effect of (a) Air Pressure and (b) Tool Offset on surface roughness and material removal

5.3 Effect of polishing time

The effect of polishing time on surface roughness and material removal was quantitatively evaluated and the results were summarized in Fig.8. It was observed that the surface roughness was not reduced any further beyond the polishing time of 12mins. The reason behind the increase in surface roughness after 12mins was due to the abrasive size, approximately 1μm, which is unable to continue to eliminate scratches. In Fig.8(b), the material removal increases with time progression, but not in linear relationship. This may be attribute to the fact that over polishing time, SiC particles continue to scratch the surface of the bearing steel, causing the wear of abrasives and was thusly represented in material removal.

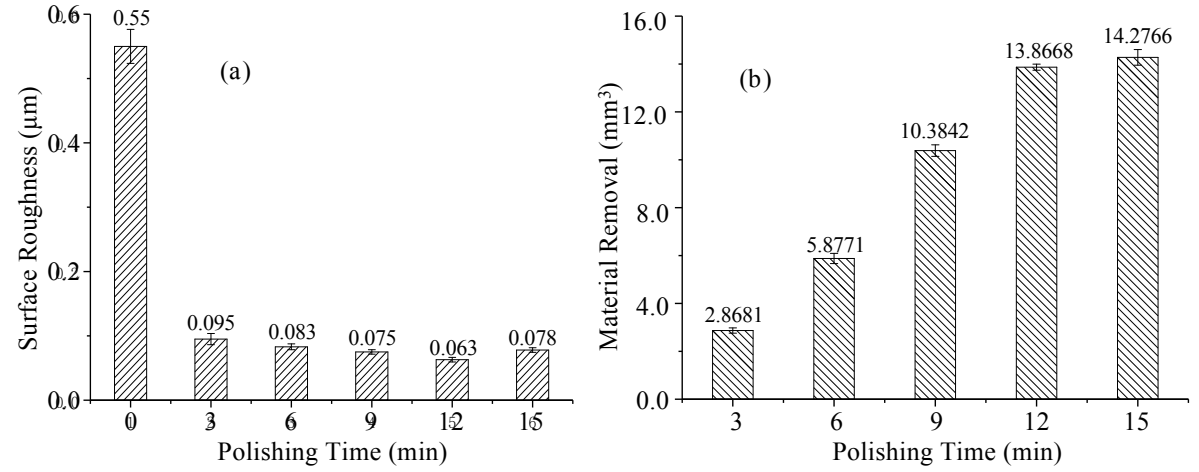

Fig.8 Effect of polishing time on surface roughness and material removal

5.4 Effect of rotation speed

The results of the surface roughness and material removal against different rotation speeds were concluded in Fig.9. As shown in Fig.9(a), the surface roughness decreases rapidly with the change of rotation speed and gradually increases after 1500rpm. On the other hand, the material removal increased with rotation speed, in Fig.9(b). The results indicated that low rotation speed generated a rough surface roughness and a low material removal while high rotation speed resulted in a high material removal. However, low rotation speed can also be adopted in fine polishing because of the low material removal.

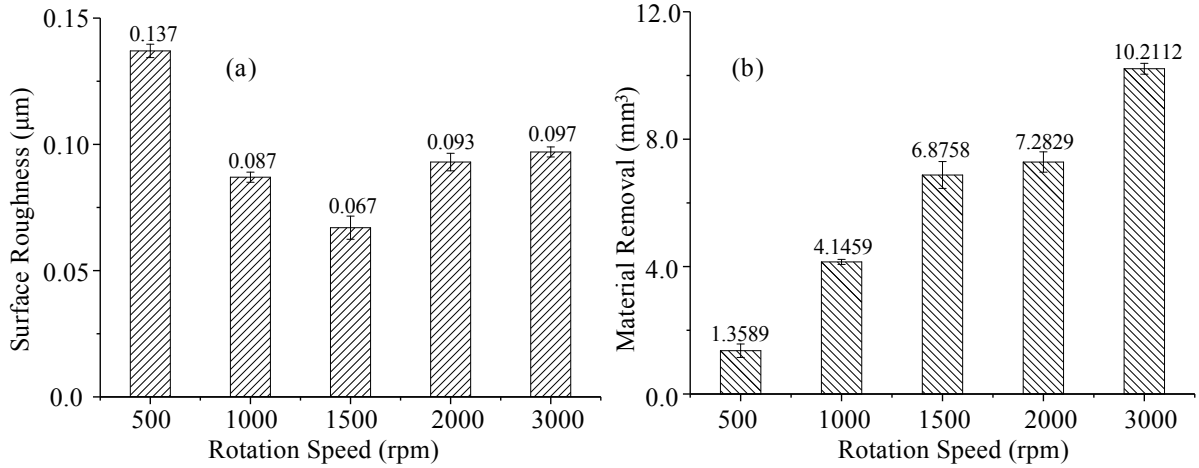

Fig.9 Effect of rotation speed on surface roughness and material removal

5.5 Effect of abrasives

The effect of abrasives on surface roughness and material removal was quantitatively evaluated by different combination of abrasives shown in Table.1. The results were summarized in Fig.10. For different abrasive combinations, it can be observed that the surface roughness drops rapidly in 12 mins polishing time. And the lowest roughness was achieved at the 1μm SiC+0.5μm CeO_2 combination conditions, about 0.0265μm in Fig.11. The reason behind better surface roughness was due to the high-speed scratching of the workpiece surface by the high-hardness SiC particles (HM9.2) within the first 6 mins, the majority of scratches were removed, and the fine polishing at low-speed by the lower hardness CeO_2 (HM6) particles in the second six minutes to improve the quality of the surface.

On the other hand, the material removal results are not in linear relationship. This is due to the different particle hardness and particle size. When using the same size particles, SiC particles lead to higher material removal compared to CeO_2 particles. In the process of combination polishing, the material removal for the combination of 1μm SiC and 0.5μm CeO_2 particles is lower than that pure SiC particles, while the material removal of pure CeO_2 particles is lowest.

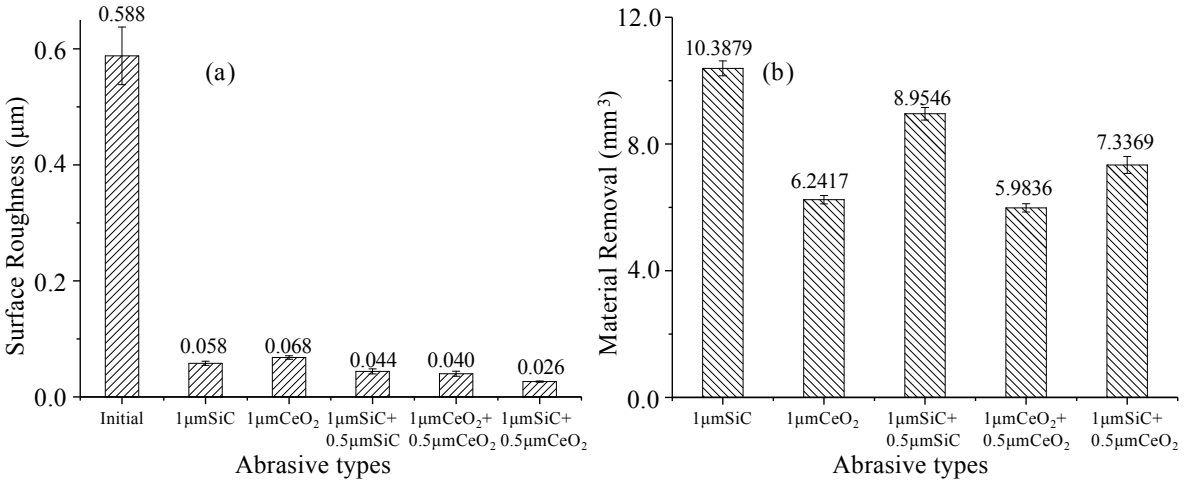

Fig.10 Effect of abrasive types on surface roughness and material removal

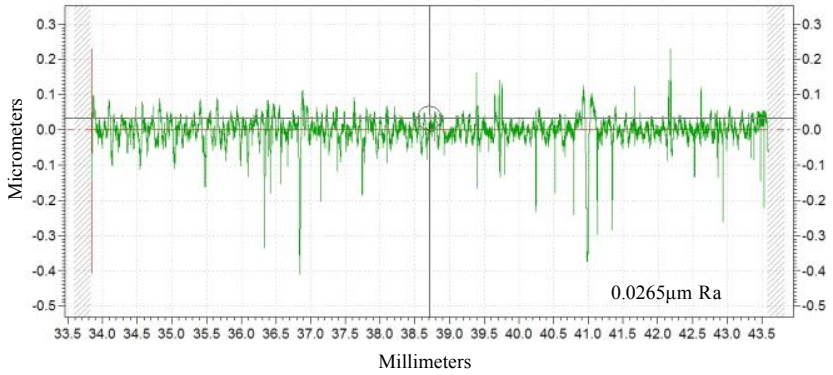

Fig.11 Surface roughness under 1μm SiC+0.5μm CeO_2 combination conditions

Fig.12 shows the three-dimensional surface images of the initial surface of the workpiece and the surface after 12mins polishing by using the 1μm SiC and 0.5μm CeO_2 abrasives. Fig.12(a) show that the scratches of the initial surface were highly apparent, and the surface was microscopically concave and convex. After 12mins of polishing using CBTP method, the scratches and asperities on the workpiece surface were no longer visible.

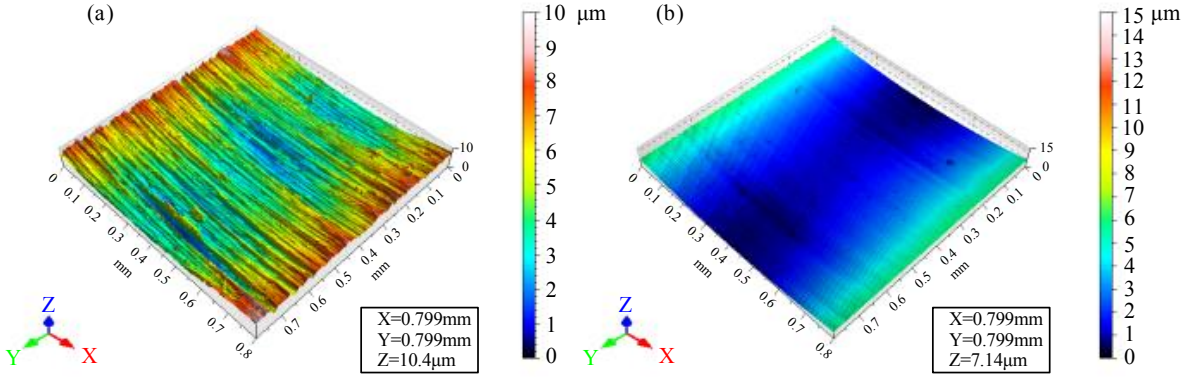

Fig.12 Three-dimensional surface topography: (a) Before polishing; (b) After polishing

6 Conclusion

In this paper, a novel CBTP method and its tool are proposed, which attempt to process the internal surface of bearing ring. The mechanism analysis demonstrate that this method can

polish the internal surface of cylindrical workpiece. Simulation experiments prove that proper inner air pressure and tool offset will be helpful in enhancing the stability of pressure distribution in the contact area. Moreover, single factor experiments have been conducted to investigate the processing capability for improving surface quality. Experimental results show that the combining rotation and reciprocating motion modes can improve surface roughness while eliminating scratches simultaneously. Higher air pressure (0.3MPa) and proper tool offset (0.1mm) is conducive to improve surface roughness and polishing efficiency, which is consistent with simulation results. In addition, a longer polishing time and a faster rotation speed can largely improve the polishing efficiency and the better surface roughness can be achieved at 1500rpm. On the other hand, the surface roughness can be achieved 0.0265μm by using 1μm SiC and 0.5μm CeO_2 particles. Hence, the CBTP method is becoming a promising and controllable method to polishing the internal surface of cylindrical workpieces. In addition, it can also be used for polishing the external surfaces.

Reference

[1] LL Cui, X Wang, HQ Wang, JF Ma. Research on Remaining Useful Life Prediction of Rolling Element Bearings Based on Time-Varying Kalman Filter. Ieee Transactions on Instrumentation and Measurement, 69 (2020) 2858-2867.

[2] H Wang, XC Liu, CJ Liu, WX Li. A New Strengthening-Polishing Bearings Equipment Based on the Anti-Fatigue Manufacturing Technology. Advanced Materials Research, 328-330 (2011) 2211-2214.

[3] SR Agha, CR Liu. Experimental study on the performance of superfinish hard turned surfaces in rolling contact. Wear, 244 (2000) 52-59.

[4] N Jouini, P Revel, G Thoquenne. Influence of surface integrity on fatigue life of bearing rings finished by precision hard turning and grinding. Journal of Manufacturing Processes, 57 (2020) 444-451.

[5] Z Chang, L Hu. Investigating the influence of the superfinishing process on the residual stress of the raceway. Transactions of the Canadian Society for Mechanical Engineering, (2022).

[6] M Li. Material Removal Mathematics Model of Shear Thickening Polishing. Journal of Mechanical Engineering, 52 (2016).

[7] M Li. Surface integrity of bearing steel element with a new high-efficiency shear thickening polishing technique. 4th CIRP Conference on Surface Integrity, (2018).

[8] M Li, F Song, Z Huang. Control strategy of machining efficiency and accuracy in weak-chemical-coordinated-thickening polishing (WCCTP) process on spherical curved 9Cr18 components. Journal of Manufacturing Processes, 74 (2022) 266-282.

[9] ATH Beaucamp, K Nagai, T Hirayama, M Okada, H Suzuki, Y Namba. Elucidation of material removal mechanism in float polishing. Precision Engineering-Journal of the International Societies for Precision Engineering and Nanotechnology, 73 (2022) 423-434.

[10] DN Nguyen, NL Chau, T-P Dao, C Prakash, S Singh. Experimental study on polishing process of cylindrical roller bearings. Measurement and Control, 52 (2019) 1272-1281.

[11] CH Zhao, NS Qu, XC Tang. Electrochemical mechanical polishing of internal holes created by selective laser melting. Journal of Manufacturing Processes, 64 (2021) 1544-1562.

[12] J Zhang. Experimental and theoretical study of internal finishing by a novel magnetically

driven polishing tool. Machine Tools & Manufacture (2020).
[13] RW Mccarty, Method of honing by extruding, in, 1970.
[14] MY Wu, H Gao. Experimental study on large size bearing ring raceways' precision polishing with abrasive flowing machine (AFM) method. The International Journal of Advanced Manufacturing Technology, 83 (2015) 1927-1935.
[15] BS Brar, RS Walia, VP Singh. Electrochemical-aided abrasive flow machining (ECA2FM) process: a hybrid machining process. The International Journal of Advanced Manufacturing Technology, 79 (2015) 329-342.
[16] AP Nagalingam, VC Thiruchelvam, SH Yeo. A novel hydrodynamic cavitation abrasive technique for internal surface finishing. Journal of Manufacturing Processes, 46 (2019) 44-58.
[17] M Das, VK Jain, PS Ghoshdastidar. A 2D CFD simulation of MR polishing medium in magnetic field-assisted finishing process using electromagnet. The International Journal of Advanced Manufacturing Technology, 76 (2014) 173-187.
[18] Z Fan, Y Tian, Z Liu, C Shi, Y Zhao. Investigation of a novel finishing tool in magnetic field assisted finishing for titanium alloy Ti-6Al-4V. Journal of Manufacturing Processes, 43 (2019) 74-82.
[19] Z Peng, W-L Song, C-L Ye, P Shi, S-B Choi. Model establishment of surface roughness and experimental investigation on magnetorheological finishing for polishing the internal surface of titanium alloy tubes. Journal of Intelligent Material Systems and Structures, 32 (2020) 1278-1289.
[20] W Song, Z Peng, P Li, P Shi, SB Choi. Annular Surface Micromachining of Titanium Tubes Using a Magnetorheological Polishing Technique. Micromachines (Basel), 11 (2020).
[21] W-C Chen, K-L Wu, B-H Yan, M-C Tsao. A study on the magneto-assisted spiral polishing on the inner wall of the bore with magnetic hot melt adhesive particles (MHMA particles). The International Journal of Advanced Manufacturing Technology, 69 (2013) 1791-1801.
[22] DD Walker, D Brooks, A King, R Freeman, R Morton, G McCavana, SW Kim. The 'Precessions' tooling for polishing and figuring flat, spherical and aspheric surfaces. Opt Express, 11 (2003) 958-964.
[23] DD Walker, A Beaucamp, C Dunn, R Freeman, D Riley, First results on free-form polishing using the Precessions process, in: Aspe Conference, 2004.
[24] DD Walker, G Yu, H Li, W Messelink, R Evans, A Beaucamp. Edges in CNC polishing: from mirror-segments towards semiconductors, paper 1: edges on processing the global surface. Opt Express, 20 (2012) 19787-19798.
[25] G Yu, DD Walker, H Li. Implementing a grolishing process in Zeeko IRP machines. Appl Opt, 51 (2012) 6637-6640.
[26] R Pan, B Zhong, D Chen, Z Wang, J Fan, C Zhang, S Wei. Modification of tool influence function of bonnet polishing based on interfacial friction coefficient. International Journal of Machine Tools and Manufacture, 124 (2018) 43-52.
[27] R Pan, W Zhao, B Zhong, D Chen, Z Wang, C Zha, J Fan. Evaluation of removal characteristics of bonnet polishing tool using polishing forces collected online. Journal of Manufacturing Processes, 47 (2019) 393-401.
[28] X Su, P Ji, Y Jin, D Li, D Walker, G Yu, H Li, B Wang. Simulation and experimental study on form-preserving capability of bonnet polishing for complex freeform surfaces.

Precision Engineering, 60 (2019) 54-62.